HfO_2 High-*k* Dielectric Layers in Air-Coupled Capacitive Ultrasonic Transducers

Sean G. McSweeney and William M. D. Wright

Department of Electrical and Electronic Engineering, University College Cork, Ireland
seanmcs@rennes.ucc.ie, bill.wright@ucc.ie

***Abstract*— For air-coupled applications, broadband capacitive ultrasonic transducers (CUTs) at the mm to cm scale are often desirable. Improved device performance may be obtained by etching well-defined geometric features into a silicon backplate electrode, then using a metallized polymer film as the other electrode. The use of additional dielectric coatings for devices at this scale may have a number of beneficial effects. This work investigates the use of HfO_2 high-*k* dielectric coatings on the backplate electrodes of air-coupled CUTs. A range of such devices was constructed and used in a through-transmission configuration. Different thickness HfO_2 layers were investigated at different bias voltages, and the effects on the sensitivity and bandwidth of the devices were analyzed. The predicted capacitance of each device was within 7% of the measured capacitance, with variations due to additional trapped air and manual assembly. Increasing the HfO_2 layer thickness decreased the overall capacitance of the CUT as expected, but produced significant improvements in device sensitivity and bandwidth at certain bias voltages. A strong correlation between HfO_2 high-*k* dielectric layer thickness and peak-to-peak amplitude was observed. The variation in device operation after successive bias charge/discharge cycles also become consistently less as the HfO_2 layer thickness was increased.**

***Index Terms*— High-*k* dielectric, capacitive ultrasonic transducer, air coupled ultrasound, hafnium oxide**

I. Introduction

The two most common methods of generation and detection of air-coupled ultrasound are piezoelectric and capacitive. Piezoelectric devices tend to be highly durable, but may suffer from a significant acoustic impedance mismatch when coupling to air and require impedance matching layers resulting in resonant devices, or a modified low impedance piezoelectric element.

Capacitive devices typically have a high coupling efficiency and may be less durable, although devices that operate in extreme conditions have been demonstrated [1]. A capacitive ultrasonic transducer (CUT) is essentially a parallel-plate capacitor, with one fixed rigid electrode (the backplate) and one movable flexible electrode (the membrane) typically a metallized dielectric polymer, with a thin air gap or cavity in between. The basic structure of a CUT is shown in Fig. 1.

This work was supported by a Government of Ireland IRCSET scholarship under the Embark Initiative, SFI Research Frontiers Program grant 11/RFP/ECE3119, and NAP 225 in the Tyndall National Institute, UCC.

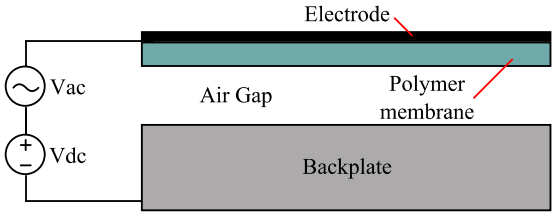

Fig. 1. Basic schematic of CUT

Typically, a dc bias voltage is applied between the two electrodes to build up charge between them. When operating as a transmitter, a superimposed voltage oscillating at the desired ultrasonic frequency causes the charge between the two electrodes to vary, and displaces the membrane to generate ultrasound; similarly when operating as a receiver, an ultrasonic wave striking the membrane causes it to displace, and produces a detectable change in charge between the membrane and backplate. The surface features of the backplate electrode heavily influence the sensitivity and frequency response of the device, but these features can be difficult to control.

Capacitive micromachined ultrasonic transducers (CMUTs) [2] typically consist of a polysilicon, Si_3N_4 or SiO_2 membrane electrode suspended over a substrate electrode, with the intervening gap produced by removal of a sacrificial layer. Due to the tight dimensional control, these devices are highly efficient but difficult to produce larger than a few tens of microns, often due to residual stress in the larger area membranes [3]. Small devices tend to be highly resonant in air, which compromises their use in applications where broadband large area devices may be more desirable.

A proven and effective compromise is to etch small well-defined geometric features in a silicon backplate electrode using standard bulk micromachining processes, then apply a commercially available metalized polymer membrane or metal foil as the other electrode to produce devices in the mm to cm scale [4].

The use of additional dielectric coatings for devices at this scale may have a number of benefits. This work investigates the use of HfO_2 high-*k* dielectric layers deposited on top of the silicon backplate electrode and the effects that these will have on the transducer operation.

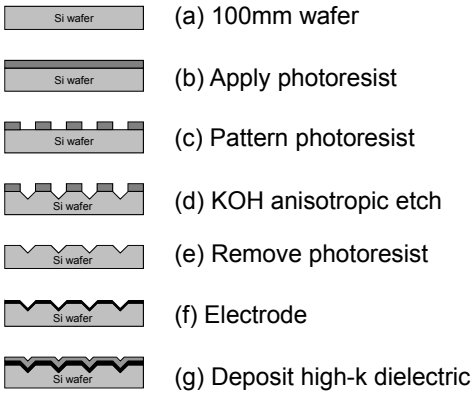

Fig. 2. Fabrication process steps for the backplates.

II. Design, Modeling and Characterization

A. Fabrication

A series of etched, electroded and coated (100) silicon wafers were manufactured as shown schematically in Fig. 2. Initially a photoresist layer was applied to the bare substrate (b) and this was then patterned with a UV source (c). A standard anisotropic KOH (potassium hydroxide) etch was then used to produce pyramidal pits with sloping sides and a self-limiting depth (d). The photoresist was then removed (e) and the backplate electrode deposited (f). Finally the HfO_2 high-k layer was deposited (g) to thicknesses of 0.2µm, 0.4µm, 0.6µm, 0.8µm and 1.0µm. The mask pattern (c), electrode (f), and high-k dielectric layer (g) were applied uniformly across the entire wafer. The metal used for the electrode was platinum due to its excellent conductivity and CMOS compatibility. No passivation layer was required.

The mask pattern consisted of a regular grid of 40µm square holes with 80µm between centers, and a SEM image of the etched pit pattern can be seen in Fig. 3. For the purposes of this work, variation of the pit geometry was assumed negligible. The wafer was then cut into 16mm square sections and assembled with a 5µm PET membrane into a screened transducer casing with a 10mm diameter aperture.

B. Device Modeling

The pits were symmetric square pyramids of edge length γ, separation distance β and sidewall incline α. A schematic cross-section of the assembled devices can be seen in Fig. 4. Similar backplate features have been modeled previously [5] using a standard equivalent circuit model.

TABLE I
Parameters of the High-K Device

PARAMETER	VALUE
Pit angle, α	125.264°
Pit pitch, β	80 µm
Pit edge length, γ	40 µm
Backplate edge length, d	16 mm
Sound speed in air, c	343 ms^{-1}
Density of air, ρ_0	1.2251 kgm^{-3}
Permittivity of free space, ε_0	8.854 pF/m
Permittivity of HfO_2, ε_k	25
Permittivity of PET, ε_m	3.4
Receiver frequency, f_0	250 kHz
Receiver Q factor	2
Number of pits, N	2704

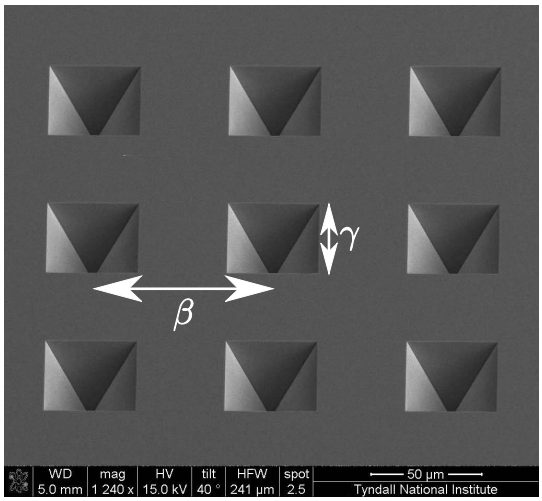

Fig. 3. SEM image of fabricated backplates.

An estimate of the resonant frequency of this pitted architecture may be determined from Helmholtz resonance theory in a similar manner to v-grooved devices [6, 7], using the membrane mass density σ and pit height h:

$$f_0 = \frac{c}{\pi}\sqrt{\frac{\rho_0}{2\sigma h}}. \tag{1}$$

Accurately predicting the capacitance of these devices is of merit as it gives a measure of the expected sensitivity of the devices. The capacitance of this pitted architecture is given by the parallel combination of the compound pit capacitances and the capacitance of the non-vibrating region of the device:

$$C = N\left(\varepsilon_0 \int_0^{\gamma/2} 8\tan(\alpha - \pi/2)\,//\,\frac{\varepsilon_0\varepsilon_k\gamma^2}{t_k}\,//\,\frac{\varepsilon_0\varepsilon_m\gamma^2}{t_m}\right) + \left(\frac{\varepsilon_0\varepsilon_k(d^2 - N\gamma^2)}{t_k}\,//\,\frac{\varepsilon_0\varepsilon_m(d^2 - N\gamma^2)}{t_m}\right), \tag{2}$$

where the parameters used in this work are shown in Table I.

C. Experimental Layout

The experimental layout of the characterization system used in this work can be seen in Fig. 5. The Panametrics 5800

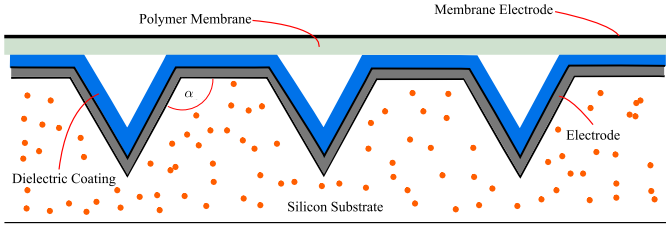

Fig. 4. Schematic cross-section of the CUT

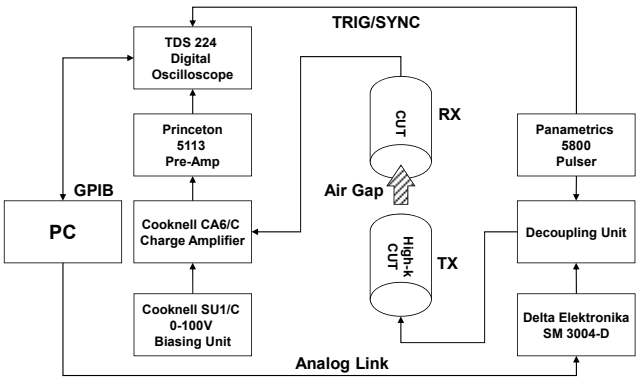

Fig. 5. Experimental layout of the testing system

supplied a pulse energy of 12.5µJ to the high-*k* CUT transmitter, with the dc bias voltage from the Delta Elektronika SM 3004-D stepped up to 300V in 256 increments. The air-coupled ultrasound was detected using a second CUT receiver with a polished metal backplate. Signals were digitized on a Tektronix TDS 200 series oscilloscope via a Cooknell CA6/C charge sensitive amplifier with a SU1/C 100V biasing unit with an additional 10dB of gain from a Princeton 5113 pre-amp. MATLAB© was used for overall system coordination, data collation and processing.

III. Results and Discussion

A number of studies were conducted to assess the effects of the different thickness high-*k* HfO_2 dielectric layers. It was speculated that there may be a number of advantages due to the additional free charge that would be available on the membrane. A number of interesting effects were observed.

The capacitance of each CUT was obtained from the average of three test runs where the RC time constant curve for an applied step response of 20V with a constant dc bias of 100V was measured. The expected capacitance of each device with a different HfO_2 layer thickness was calculated using (2);

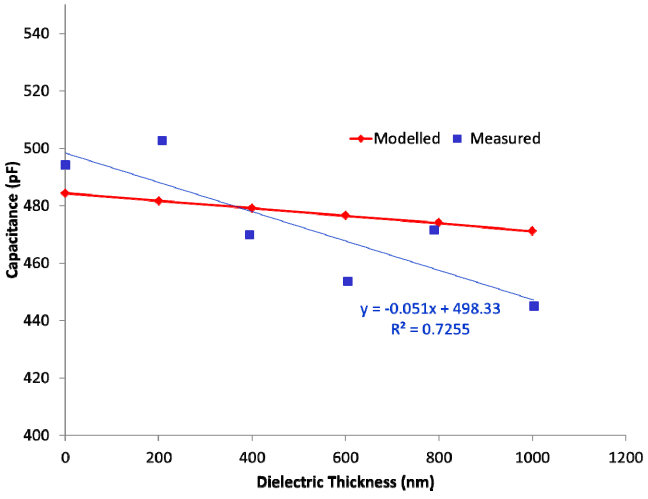

Fig. 6. Modeled and measured capacitance variation with HfO_2 high-*k* dielectric layer thickness.

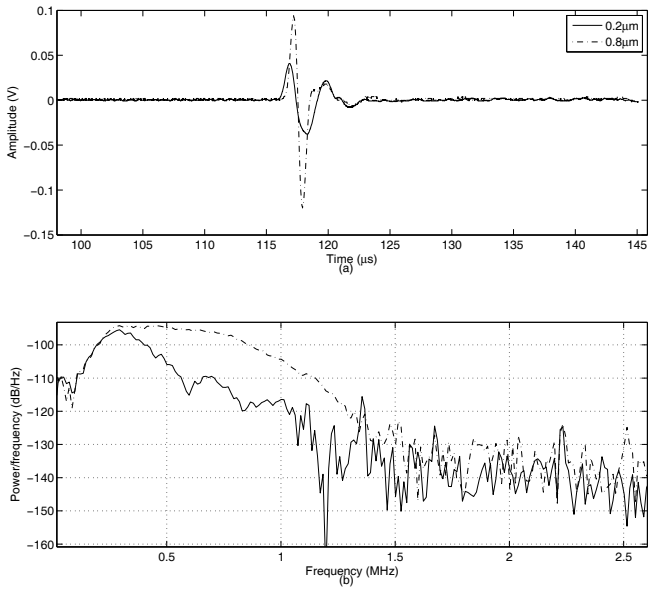

Fig. 7. Impulse (a) transient and (b) frequency domain responses of 0.2µm and 0.8µm thickness HfO_2 layer CUTs.

this is plotted in Fig. 6 against the experimentally measured capacitance. The variation between the calculated capacitance based on (2) and the measured capacitance for each thickness of high-*k* layer was less than 7%. These variations were most likely due to excess air trapped between membrane and backplate, and other minor assembly variations. The predicted resonant frequency from (1) was 211kHz and the peak response of the 0.2µm layer device is 296kHz in Fig. 7(b).

The sensitivity and bandwidth was also seen to improve as the thickness of the high-*k* layer increased. Time domain waveforms and their corresponding frequency spectra are shown in Fig. 7 (a) and (b), respectively, for 0.2µm and 0.8µm HfO_2 layer thickness as representative examples. The 0.8µm device had a peak-to-peak amplitude 8.72dB greater than the 0.2µm device, a center frequency 66% higher at 492kHz, and a *Q*-factor of 0.9. This suggests that increasing the HfO_2

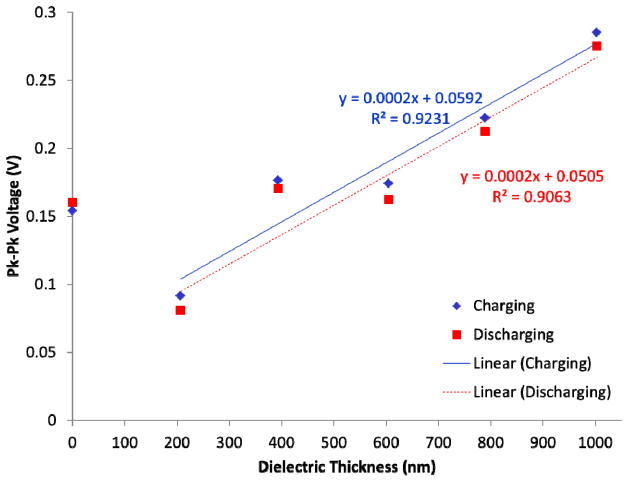

Fig. 8. Peak-to-peak amplitude of charging and discharging cycles, with best fit linear trends to each.

thickness, while decreasing the overall capacitance of the CUT, still resulted in significant benefits.

The maximum peak-to-peak amplitude of the dc bias charging and discharging cycles are displayed in Fig. 8, where a strong correlation between high-*k* dielectric thickness and sensitivity is evident. It is interesting to note that the devices with a HfO_2 layer less than 0.6µm thick appear to offer no sensitivity improvement over a device with no high-*k* layer; it is likely that the thicker high-*k* layers are more resistant to tunneling and prevent polarization of the PET membrane.

Fig. 9 and Fig. 10 show the dc bias sweeps (charging and discharging) for the 0.2µm and 0.8µm layer devices as representative examples. The first charging cycle of all devices was ignored as excess air was being forced out from between the PET membrane and backplate. There was significant variation in both the maximum peak-to-peak voltage and the bias voltage at which this occurs, between successive bias charging and discharging cycles, for all HfO_2 layer thicknesses below 0.6µm, as shown in Fig. 9 for the 0.2µm HfO_2 layer device, and the effect reduced as the layer thickness increased. These variations were most pronounced in the device with no HfO_2 layer, which demonstrated that this was most likely due to charge injection and polarization in the PET membrane. With HfO_2 layers thicker than 0.6µm, there was little or no variation between successive charging and discharging cycles, as can be seen in Fig. 10 for the 0.8µm HfO_2 layer device, and a higher sensitivity, as seen in Fig. 8.

IV. Conclusions and Future Work

As can be seen from the preliminary results presented in this work, there are significant differences in performance of the CUTs with a HfO_2 high-*k* dielectric layer that depend on the layer thickness. It would appear that there are few benefits to using HfO_2 layers less than 0.6µm thick on backplate structures such as those used in this work. Consistency of device operation appears to be improved from first charging with thicker HfO_2 layers, and the PET membrane devices may

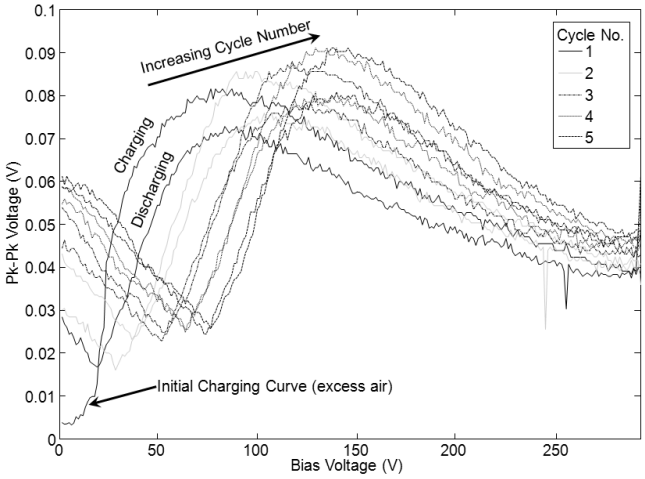

Fig. 9. Peak-to-peak amplitude for 0.2µm thickness HfO_2 dielectric layer for 5 successive bias charge/discharge cycles up to 300V.

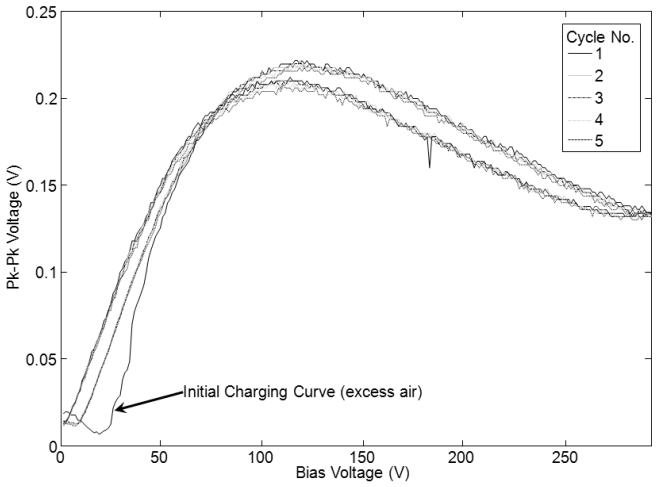

Fig. 10. Peak-to-peak amplitude for 0.8µm thickness HfO_2 dielectric layer for 5 successive bias charge/discharge cycles up to 300V.

be biased to a higher voltage without deleterious charging effects and polarization occurring in the membrane.

Variation in device capacitance was as expected to within 7%, and the results showed that despite an overall decrease in device capacitance, the sensitivity and bandwidth of the devices increased with the thickness of HfO_2 high-*k* dielectric layer used. The hysteresis variation of the devices in bias voltage charging and discharging between successive cycles was reduced, producing more consistent device characteristics and operation. Future work will investigate the use of other high-*k* dielectric materials, and modeling of charge migration in the PET and high-*k* layers.

Acknowledgments

The authors would like to thank Michael O'Shea and Timothy Power in the Department of Electrical and Electronic Engineering, UCC, and Conor O'Mahony in the Tyndall National Institute for their contributions to this work.

References

[1] A. Schroder, S. Harasek, M. Kupnik, M. Wiesinger, E. Gornik, E. Benes and M. Groschl , "A capacitance ultrasonic transducer for high-temperature applications", *IEEE Trans. UFFC*, vol.51, pp.896-907, 2004.

[2] O. Oralkan, A.S.Ergun, J.A. Johnson, M. Karaman, U. Demirci, K. Kaviani, T.H. Lee and B.T. Khuri-Yakub, "Capacitive micromachined ultrasonic transducers: Next-generation arrays for acoustic imaging?", *IEEE Trans. UFFC*, vol. 49, pp. 1596-1610, 2002.

[3] G.G. Yaralioglu, A.S. Ergun, B. Bayram, T. Marentis and B.T. Khuri-Yakub, "Residual stress and Young's modulus measurement of capacitive micromachined ultrasonic transducer membranes", *IEEE International Ultrasonics Symposium*, 2001, vol.2, pp.953-956.

[4] D.W. Schindel, D.A. Hutchins, L. Zou, and M. Sayer, "The design and characterization of micromachined air-coupled capacitance transducers", *IEEE Trans. UFFC*, vol. 42, pp. 42-50, 1995.

[5] K. Suzuki, K. Higuchi and H. Tanigawa, "A silicon electrostatic ultrasonic transducer", *IEEE Trans. UFFC*, vol. 36, pp. 620-627, 1989.

[6] M. Rafiq and C. Wykes, "The performance of capacitive ultrasonic transducers using v-grooved backplates", *Meas. Sci. Technol.*, vol. 2, pp. 168-174, 1991.

[7] J. Hietanen. J. Stor-Pellinen and M. Luukkala, "A model for an electrostatic ultrasonic transducer with a grooved backplate", *Meas. Sci. Technol.*, vol. 3, pp. 1095-1097, 1992.